ELSEVIER

High temperature reduction with hydrogen, phase composition, and activity of cobalt/silica catalysts

Janusz M. Jabłoński,* Janina Okal, Danuta Potoczna-Petru, and Ludwina Krajczyk

W. Trzebiatowski Institute of Low Temperature and Structure Research, Polish Academy of Sciences, PO Box 1410, 50-950 Wroclaw 2, Poland

Abstract

The evolution of the morphology, phase composition, and activity in benzene hydrogenation of Co/SiO_2 catalysts, prepared from cobalt nitrate and porous (390 m^2/g) or nonporous (35 m^2/g) silica, upon reduction with hydrogen at 350–900 °C have been studied by X-ray diffraction (XRD), transmission electron microscopy (TEM), magnetic measurements, oxygen uptake, BET, and hydrogen chemisorption. A rapid decline of the activity of Co/SiO_2 catalysts to zero was observed with reduction temperature increasing from 400 to 600 °C. This effect could not be simply explained by a sintering of cobalt particles or by the reaction of Co with the support and alloys or compound formation. The TEM, H_2 chemisorption, O_2 uptake, and magnetic measurements revealed that at $T_{red} \geqslant 500$ °C coverage (encapsulation) of the metal with a thin, most probably SiO_2, overlayer was likely to be the reason. Both Co/SiO_2 catalysts reduced at $T_{red} > 500$ °C exhibited a higher and growing with reduction temperature resistance to oxidation when exposed to oxygen or air as it was evidenced by oxygen uptake, magnetic data, and decreasing H_2 chemisorption capacity. At higher temperature ($\geqslant 700$ °C) the formation of a thicker, easily observable with TEM, SiO_2 or SiO_x, overlayer covering the Co particles took place. As a consequence, the catalysts reduced at 900 °C were nearly insensitive to the exposure to air. Oxygen uptake and magnetic measurements ruled out the hypothesis on the Co–Si solid solution or cobalt silicide formation at least in quantities higher than the reliability limits of the experimental methods used. The sintering of Co particles and the significant growth of the mean size of Co crystallites was observed at reduction temperatures of 800 and 850 °C for nonporous and porous silica, respectively. An apparent growth of the cobalt content to 107 and 114% of the initial value was noted after reduction at 700 and 900 °C, respectively, for both catalysts studied, probably due to the strong support dehydroxylation and/or partial reduction.
© 2003 Elsevier Inc. All rights reserved.

Keywords: Co/SiO_2 catalysts; High-temperature reduction; Benzene hydrogenation; Hydrogen chemisorption; Oxygen uptake; Magnetism; TEM; Co encapsulation

1. Introduction

Supported cobalt has been extensively studied as catalyst for the reactions involving hydrogen transfer. The best-known industrial scale application is the Fischer–Tropsch reaction in which cobalt-based catalysts are used [1–3]. Other promising reactions studied were carbon dioxide reforming of methane [4], ethene hydroformylation [5], hydrogenation of aromatics [6–8], and selective hydrogenation of aldehyde groups in α, β-unsaturated aldehydes [9]. It is well known that the reduced cobalt metal, rather than its compounds like carbides, is the active phase for hydrogenation and Fischer–Tropsch reactions. For structurally insensitive reactions, only two factors, in principle, determine an effec-

tive use of a metal precursor in a catalyst and as a consequence the catalyst activity, namely degree of its reduction and the shape and dimensions of metal particles formed.

It has been shown that the reducibility of the cobalt catalysts and, in general, the dispersion of the metal phase formed depend on the support used [10–20]; the cobalt precursor used [15,17,21–24]; the metal loading [8,11,18], the preparation method [11,14,17,25–29]; thermal treatment [15,21,30–32], the reduction process [33–35], and also the added ions [36–40]. All above-noted factors seem to reflect different nanoscale chemistry at the interface in each particular case. Recently much attention was paid, to the study of the influence of the catalyst preparation and thermal treatment (drying/calcination) steps and also the reduction process itself, on the activity of the resulting cobalt catalysts. The two former steps can produce irreducible or resistant to reduction compounds formed from metal precursor and the

---

* Corresponding author.
E-mail address: janusz@int.pan.wroc.pl (J.M. Jabłoński).

support. The last step can strongly influence the final state or composition of the metallic phase formed and hence also the activity.

Although silica was generally considered as a relatively inert support [41,42], it was found that cobalt species deposited on silica support could, under certain experimental conditions, partly or fully react with the support. The reaction may lead to only a partial reduction of cobalt and a lower activity of the resulting catalyst. Puskas et al. [14] found that preparation of the precipitated cobalt on silica catalysts, in a slightly alkaline reaction environment, resulted in cobalt silicate formation which could be reduced only at elevated temperatures (i.e., above 500 °C). Ming and Baker [26] reported on the influence of pH of the impregnating solution on the formation of cobalt silicate in cobalt silica-gel catalysts. The cobalt silicate formation in the Co/SiO_2 catalyst has been shown to enlarge with increasing surface area of the support [14,15]. Recently, Barbier et al. [28] reported two-dimensional cobalt phyllosilicate formation in well-dispersed Co/SiO_2 catalysts prepared by the ammonia method.

It was shown that the reducibility of cobalt could be strongly influenced by the drying procedure [15,30,32]. High-temperature calcination, both in oxygen and in an inert atmosphere, can produce silicate, which is difficult to reduce [15,26,30,31,43–45]. It was found that even reduced cobalt is able to produce silicate or hydrosilicate under hydrothermal conditions [31]. Reaction of Co/SiO_2 with high-pressure steam at 220 °C leads to a substantial loss of BET surface area and formation of catalytically inactive cobalt silicate [46]. Similar effects have been observed after repeated aqueous impregnation of the prereduced and passivated Co/SiO_2 catalysts during drying [45] or calcining [44]. On the other hand, cobalt silicate formation can act as a beneficial factor. It has been postulated that a small amount of this compound is necessary to obtain a highly dispersed cobalt catalyst [30].

The reduction process itself strongly influences the quality of the resulting catalyst. It is well known that the catalytic activity of the catalyst can be suppressed by the so-called strong metal support interaction (SMSI) effect, which occurs during the reduction step at higher temperatures [47,48]. Formation of the intermetallic compounds in the metal/transition metal oxide systems, accompanied with the suppression of the catalytic activity in benzene hydrogenation, has been reported some time ago for Ni/ZnO [49] and Pd/ZnO [50]. Later it was shown that even supports considered earlier as inert ones can undergo reduction at higher temperatures in the presence of active metals with the formation of compounds or alloys, as it was observed, for example, in Ni/SiO_2 [51], Ni/Al_2O_3 [52], Pt/SiO_2 [53], and Pd/SiO_2 [35,54,55] catalysts. On the other hand, partly reduced support moieties [8] or the support itself [56], migrating onto the metal particles, can lower the catalytic activity. The reduction conditions, in particular the water vapor, strongly influence the reducibility and activity of cobalt cat-

alyst, as it was shown by Goodwin and co-workers [33,34] for $Co,Ru/Al_2O_3$ catalysts. The presence of water vapor can also influence the phase composition of the final catalyst as it has been reported for Pd/SiO_2 [35].

Although the phenomenon of a strong metal support interaction has been investigated recently for model Co/SiO_2 and Co/C catalysts in the form of thin films [57,58], the literature concerning Co catalysts on porous silica supports is rather scarce [18,59,60]. Moreover, some catalytic reactions actually studied [4], employing Co/SiO_2 catalysts, take place at temperatures around 800–900 °C, so it would be desirable to have a better insight into the chemistry of this system also at higher temperatures.

We undertook this study to elucidate the influence of the silica support type and high-temperature reduction on the morphology, phase composition, sintering, and catalytic activity of supported cobalt catalysts. To study the effects induced by the reduction, it would be desirable to separate it from others, which would take place at the earlier stages of catalyst preparation, i.e., impregnation and calcination. Therefore, the cobalt nitrate precursor was used as it is relatively well investigated and is known to not produce a stronger interaction with silica during impregnation and under mild calcination treatment [32,61]. The supported Co catalyst based on the cobalt nitrate precursor is also often used as a reference. In the present study, to follow the change of the cobalt surface area and its metallic function, as well as phase composition, besides the transmission electron microscopy (TEM) and selected area electron diffraction (SAED), we have also adopted X-ray diffraction (XRD), hydrogen chemisorption, oxygen uptake, nitrogen adsorption, magnetic measurements, and benzene hydrogenation as a test reaction. Hydrogenation of benzene is considered to be a structure-insensitive reaction [3,62]; therefore, the reaction rate should be a good measure of the accessible cobalt surface sites.

2. Experimental

2.1. Catalyst preparation

Two types of silica from Rhône-Poulenc, denoted as XOA-400 ($S = 390$ m^2/g, pore volume 1.25 cm^3/g, mean pore diameter 100 Å) and XOB-15 ($S = 26$ m^2/g, pore volume 0.3 cm^3/g, mean pore diameter 2000 Å)—according to the manufacturer's data—were used for catalyst preparation. BET measurements performed in our laboratory gave the surface area equal to 390.6 and 35.1 m^2/g, respectively. The supports before impregnation were washed twice with doubly distilled water (DDW) and 50 $cm^3/1$ g SiO_2, filtered, and dried overnight in air at room temperature and subsequently 20 h at 200 °C. Two catalysts were prepared by incipient wetness impregnation of the supports with an appropriate amount of $Co(NO_3)_2 \cdot 6H_2O$ (supplied by POCH, Gliwice, Poland; analytical grade) DDW solutions. The catalysts were

dried in air at room temperature for 72 h followed by calcination in the open air of an oven at 130 °C for 20 h. Once prepared, the catalysts were stored in tightly closed bottles and used for experiments without any additional treatment. The catalysts will be referred to as Co/SiO_2-390 and Co/SiO_2-35 catalysts, respectively.

2.2. Chemical analysis

Elemental analysis of bare supports and catalysts was performed by using inductively coupled plasma-atom emission spectrometry (ICP-AES) with a Philips Scientific PU 7000 spectrometer. About 1 g of the support, after drying at 250 °C for 5 h, was dissolved with an appropriate amount of hydrofluoric and diluted sulfuric acids. The analysis revealed the following trace metal contents (expressed as ppm (µg/g)): SiO_2-390 support (Ca, 169; K, 13; Mg, 41; and Na, 189), SiO_2-35 support (Ca, 195; K, 16; Li, 0.9; Mg, 162; and Na, 3410). Preliminary experiments have shown that reliable determination of the cobalt contents in the catalysts necessary to achieve the purposes of this work requires the standardization of the procedures and conditions under which the analyse are made. Therefore, before analysis the catalysts were reduced with hydrogen flow at 400 °C for 5 h and then oxidized in flowing air for 3 h to convert Co into Co_3O_4. Next, the samples were dissolved with an appropriate quantity of the mixture of hydrochloric and nitric acids. The analyses revealed the following cobalt loading: 8.54 wt% Co for Co/SiO_2-390 and 4.88 wt% Co for Co/SiO_2-35 as expressed on a reduced catalysts basis. Thus, the Co loading means weight percentage Co in the completely reduced catalysts. In the case of the Co/SiO_2-35 catalyst, the amount of Co corresponds approximately to the monolayer coverage, while for the Co/SiO_2-390 catalyst to about 0.21 of a monolayer. The cobalt content in selected samples of the catalysts subjected to the oxygen uptake and magnetic measurements was also additionally determined gravimetrically via complex with α-nitro-β-naphthol according to the procedure given in Ref. [63].

2.3. Catalyst reduction and pretreatment

The reduction was performed in a similar way as described in [43]. The catalyst sample (usually 500, sometimes up to 1200 mg) placed into a quartz tube was heated in purified hydrogen flow (60 cm^3/min), with the heating rate of 5 °C/min, to the required temperature and then was maintained for 20 h. After cooling down to room temperature under flowing hydrogen, the catalyst sample was passivated by allowing air to leak slowly into the reduction tube. Sometimes for comparison purposes the catalyst was passivated with flowing 0.5% O_2 in N_2 before being exposed to air. Then, the catalyst was divided, as soon as possible, into suitable parts to be studied with the various methods used. All characterization experiments and some activity measurements were carried out ex situ, and reduced catalyst samples

were handled in air. Only the samples for magnetic measurements and for selected oxygen uptake experiments were handled under hydrogen, subsequently degassed (400 °C, 4 h, 10^{-5} Torr) and sealed off under vacuum without any contact with air unless stated otherwise.

2.4. Catalyst characterization

2.4.1. BET surface area

The volumetric experiments in this study, i.e., nitrogen adsorption, hydrogen chemisorption, and oxygen uptake were carried out in the same conventional glass apparatus providing a base pressure of 10^{-6} Torr (1 Torr = 133 N/m^2). The BET surface area of the samples was measured by nitrogen adsorption at liquid nitrogen temperature, assuming 0.162 nm^2 as the area occupied by the N_2 molecule. Before measurements the bare supports and the oxidized forms of the catalysts were degassed for 2 h at 250 °C. The reduced catalyst samples, as transferred in air, were additionally reduced in hydrogen according to the procedure given in Section 2.4.6.

2.4.2. X-ray powder diffraction

X-ray powder diffraction was performed to determine the crystalline phases of the catalysts following different pretreatment steps. XRD patterns were collected using a Siemens D 5000 diffractometer with monochromatized Cu-$K_{\alpha 1}$ radiation ($\lambda = 1.5406$ Å) in the 2θ range of 10–80°. In some experiments, to minimize the influence and to verify the importance of the fluorescence, the powder diffractometer DRON-2 (Russian) with Co-$K_{\alpha 1}$ radiation ($\lambda = 1.7092$ Å), filtered with a Fe filter was also employed. Silicon powder was added to the selected samples as an internal standard for precise measurements of lattice parameters and for instrumental peak-broadening correction for determination of mean crystallite sizes. The mean crystallite sizes of Co and Co_3O_4 were calculated using the Scherrer formula [64]. The intensities of the peaks and positions of their maxima were determined by a profile fitting procedure. The crystalline phases both in XRD and SAED studies were identified by comparison with JCPDS files: Co metal (15-0806, 05-0727), Co_3O_4 (09-0418, 42-1467), and CoO (09-0402).

2.4.3. High-resolution transmission electron microscopy

To achieve the appropriate electron transparent samples, the catalyst was crushed and ground to a fine powder in an agate mortar. A copper microscope grid covered with perforated carbon was then simply dipped into the powder and a sufficient amount of material stuck to the grid for TEM examinations. Samples were examined using a Philips CM 20 Super Twin high-resolution electron microscope at 200 keV. Selected area electron diffraction, microdiffraction, and high-resolution transmission (HRTEM) working modes were used to monitor the changes in morphology and phase composition of the catalysts. The average cobalt particle size was measured by conventional diffraction contrast imaging

and calculated using the formula $\overline{D} = \sum_i n_i = \overline{D}_i / \sum_i n_i$, where n_i is the number of particles with diameter between D_i and $D_i + \Delta D_i$, and $\overline{D}_i = D_i + \Delta D_i / 2$. A minimum of about 500 particles has been measured for each sample. Homogeneity of the active phase distribution and overall chemical composition of the samples was checked with a Philips 515 scanning electron microscope ($E = 30$ kV) equipped with an EDS analyzer.

2.4.4. Magnetic measurements

Magnetic measurements were employed primarily to verify the possible Co–Si solid solution or compounds, e.g., silicide formation. The method could also be used to determine the Co content and reduction degree in the catalysts studied. Static magnetic measurements were performed by the Faraday method in an electromagnet providing field up to 7.35 kOe (0.735 T) in the apparatus described in Ref. [65]. The specific magnetization was determined at room and liquid nitrogen temperatures. Saturation magnetization per gram of the catalyst (σ_s) was obtained by plotting the reciprocal of magnetization σ against $1/H$, where H is magnetic field intensity, and extrapolating to $1/H = 0$. Reduced catalysts for magnetic measurements were handled without any contact with air and measured after being degassed. In some cases, to verify its resistance to oxidation, we simultaneously prepared another catalyst sample exposed to air for 10 min. This sample was pumped off in a vacuum as it described in Section 2.3.

2.4.5. Oxygen uptake

The extent of cobalt reduction in selected catalyst samples was determined additionally by the oxygen uptake, according to the procedure given by Bartholomew and Farrauto [66]. The reduced, carefully passivated sample of catalyst was pretreated in the same way as in Section 2.4.6. Finally, it was additionally degassed at 450 °C for 2 h and cooled to room temperature under dynamic vacuum. Then, oxygen was admitted and the amount of adsorbed oxygen was measured. The temperature was subsequently raised up to 450 °C, kept under isothermal conditions for 2 h, and then the sample was cooled under oxygen to room temperature, where the total O_2 uptake was measured. Blank experiments with bare supports were also carried out. Also, selected samples of the catalyst were prepared without any contact with air. Previously reduced catalyst sample was transferred under hydrogen into a thin-wall glass ampoule, degassed under vacuum of 10^{-6} Torr at 450 °C for 2 h, and sealed off. Next, it was transferred to the apparatus for the oxygen uptake measurement, and after degassing at 400 °C, was broken there. In this case, the oxygen uptake measurement was performed without any additional degassing of the sample.

2.4.6. Hydrogen chemisorption

For hydrogen chemisorption, the previously reduced and passivated catalyst sample (ca. 1.0 g), after being outgassed at room temperature for 2 h, was subjected to twofold rere-

duction at 400 °C in H_2 at 200 Torr for 2 h and then evacuated at the same temperature for 2 h. Finally, the sample was cooled to 100 °C under dynamic vacuum and saturated with H_2 in the pressure range of 80–150 Torr. An equilibration time of 1 h was employed. The total chemisorption of hydrogen at 100 °C, assuming a stoichiometry of $H/Co_s = 1$, was used for cobalt metal area determination instead of irreversible one, as it was shown that it better reflects the accessible metal cobalt surface [45,67].

2.4.7. Catalytic activity measurements

The catalytic activity for the benzene hydrogenation was measured at atmospheric pressure with a feed composition of benzene (Aldrich, HPLC grade 99.9%) to hydrogen equal to 1:8.75. Usually, 50 mg (Co/SiO$_2$-35) or 15 mg (Co/SiO$_2$-390) of the catalyst was loaded into a glass reactor to keep the conversion below 15% and to avoid heat and mass transport effects. Before testing, an additional in situ reduction in hydrogen flow at 400 °C for 2 h was applied, with the exception of the catalysts previously reduced at 350 °C, where the same temperature was used. The reactor effluent was analyzed by the INCO 505 M gas chromatograph (Poland) with TCD detector and equipped with 3.7 m long 15% Carbowax 20M/Gas-Chrom Q$_1$ packed columns. Because of the initial loss of activity, the bracketing technique was employed in the kinetic runs [68]. The measurements were performed at 119 °C. Additional experiments were done to check that the exposure of the reduced catalyst to air did not change the activity data, as compared to that obtained for catalysts reduced in situ, at least within the error limit of the method used. Blank runs of the empty reactor and bare supports were also performed.

3. Results

3.1. BET surface area

BET surface areas of the bare supports and cobalt catalysts after various pretreatments are shown in Table 1. The supports subjected to heating in hydrogen up to 800 °C have a surface area slightly less than that of the untreated ones. However, the pretreatment at 900 °C causes a severe decrease of the surface area, especially large in the case of the low surface area silica. The catalysts after impregnation and heating at 130 °C, show a slightly higher surface area than

Table 1
BET surface area of the bare supports and Co/SiO$_2$ catalysts after different thermal treatments

Temperature (°C)/ gas	S_{BET}, supports (m^2/g)		S_{BET}, catalysts (m^2/g)	
	SiO$_2$-35	SiO$_2$-390	Co/SiO$_2$-35	Co/SiO$_2$-390
130/air	35.0	390.6	37.3	363.0
600/H$_2$	–	–	31.3	382.1
800/H$_2$	30.2	380.5	31.1	370.0
900/H$_2$	7.1	289.5	9.5	270.2

that of the bare support in the case of the Co/SiO$_2$-35 catalyst and slightly lower for the Co/SiO$_2$-390 catalyst, respectively. Both catalysts seem to be rather stable up to reduction temperature of 800 °C, since the surface areas are only slightly lower than that of silica supports. However, the reduction at 900 °C, similarly as for the bare supports, leads to a significant loss of the surface area, which may be responsible for some sintering of the Co phase.

3.2. X-ray diffraction

For a clearness of the presentation in Fig. 1 only XRD patterns of the Co/SiO$_2$-390 catalyst following various pretreatment steps are shown. The results obtained for the Co/SiO$_2$-35 catalyst were essentially the same, although because of a lower cobalt loading, the XRD patterns were
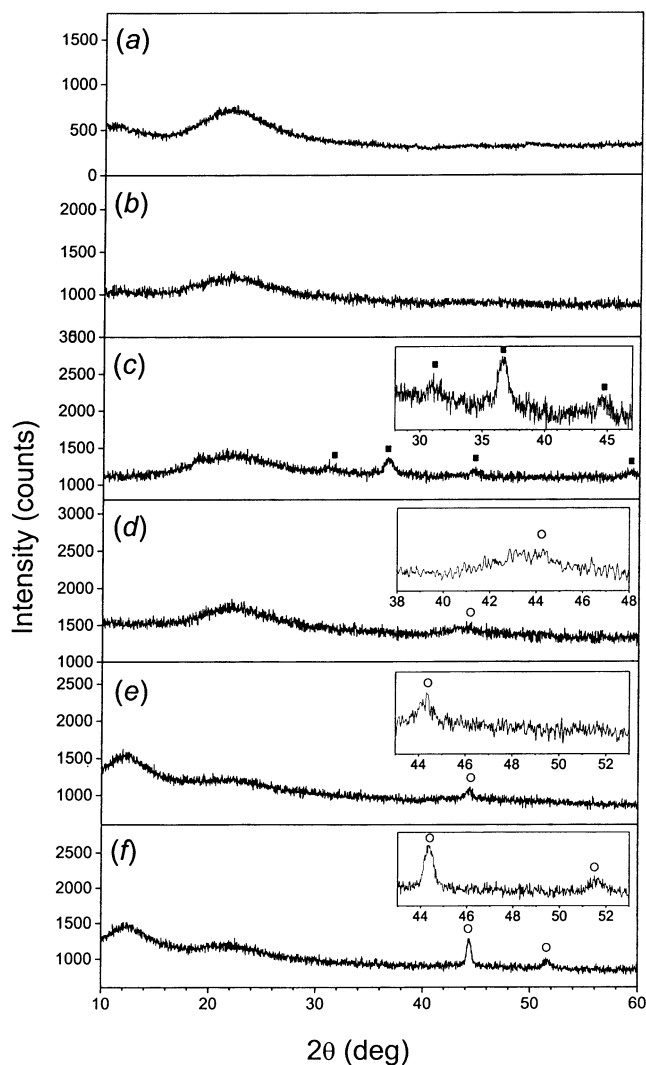

Fig. 1. Selected XRD patterns of the bare support and Co/SiO$_2$-390 after different thermal treatments. (a) SiO$_2$-390 heated in H$_2$ at 900 °C for 20 h, (b) impregnated, room temperature-dried on air for 72 h, (c) heated in air at 130 °C for 20 h and (d) catalyst reduced at 400 °C, (e) 700 °C, and (f) 900 °C. (○) fcc Co, (■) Co$_3$O$_4$. Broad peak at $2\theta = 10$–$20°$ in (e) and (f) is due to the plastic sample holder.

slightly poorer. The heating of the SiO$_2$-390 support at 900 °C in hydrogen (Fig. 1a), despite the remarkable loss of its BET surface area, did not produce any diffraction peaks which could be due to the support crystallization. Freshly impregnated with Co(NO$_3$)$_2$ and room temperature-dried silica (Fig. 1b) also did not show any diffraction peaks, which could be due to the crystalline cobalt nitrate formation. After heating in air at 130 °C only peaks, which can be ascribed to the Co$_3$O$_4$, were observed (Fig. 1c), which proved the decomposition of the cobalt nitrate. It seems that the prevailing part of the cobalt present is converted into Co$_3$O$_4$ since there is no evidence for CoO or Co$_2$O$_3$ phase formation. The mean Co$_3$O$_4$ crystallite size determined for the Co/SiO$_2$-390 catalyst from the peak at $2\theta = 36.84°$ was estimated as 9.9 nm.

In Figs. 1d, 1e, and 1f the XRD patterns of the catalyst reduced at 450, 700, and 900 °C for 20 h and exposed to air during XRD experiments are shown. After reduction at 450 °C, the diffraction peaks of Co$_3$O$_4$ disappeared and a weak broadened and diffused peak at 44.22° is observed, indicating the presence of heavily oxidized and/or highly dispersed metallic cobalt with fcc structure (β-phase). The strongest peak of CoO at 42.40° is hardly visible. The substantial oxidation of metallic cobalt and mostly amorphous cobalt oxide layer formation during the handling and XRD experiments not only confirm Co phase formation but also suggests rather good and uniform dispersion of the metallic phase. The catalyst reduced at 700 and 900 °C exhibits stronger fcc cobalt peaks, which could be interpreted as cobalt sintering and/or its greater resistance to oxidation. For the sample reduced at 900 °C, besides the stronger and narrower peak at 44.22°, also the peak at 51.52° is visible.

The use of the liquid paraffins to protect the cobalt particles from air [29,33] allowed us, however, to determine the mean sizes of cobalt crystallites (the patterns not shown here). The results are presented in Table 2, together with data obtained from TEM study. In all XRD spectra of the catalysts, both exposed to air or protected with paraffines, we have never observed the formation of the α-Co (hcp) phase. Additionally, careful determination of the peak positions in the XRD patterns, with the use of silicon powder as internal standard and a peak profile-fitting procedure, revealed a minute (by 0.26%) contraction of the Co unit cell parameter (cf. Table 2) as compared to the value of the bulk fcc Co equal to 0.3545 nm.

3.3. Transmission electron microscopy

Both TEM images and SAED patterns of freshly impregnated catalysts, after room temperature drying for 72 h, gave no evidence of the presence of amorphous or crystalline Co(NO$_3$)$_2 \times$ H$_2$O phase. In Fig. 2 TEM micrographs of the catalysts after heating at 130 °C in air are shown. The SAED patterns, presented as insets in Fig. 2, taken from the darker features (marked by arrows) could be indexed as the Co$_3$O$_4$ phase. In the case of high surface area silica

Table 2
Influence of the reduction temperature on the morphology and phase composition of Co/SiO$_2$ catalysts

Reduction temperature (°C)	Crystallite size (nm)		Co dispersion[a]	Lattice constant[b]	Phases identified[c]
	XRD	TEM	(%)	XRD (nm)	TEM
Co/SiO$_2$-390					
350	–	8.4	11.8	–	Co(*fcc, hcp*), CoO
400	–	9.9	9.8	–	Co(*fcc, hcp*), CoO
450	9.0	9.8	10.1	–	Co(*fcc, hcp*), CoO
550	–	8.1	12.3	–	Co(*fcc, hcp*)
700	6.7[d]	10.1	9.8	0.3533 (5)	Co(*fcc, hcp*)
800	–	9.1	10.8	–	Co(*fcc, hcp*)
850	15.2	16.1	6.2	–	Co(*fcc, hcp*)
900	21.1	23.5	4.2	0.3545 (5)	Co(*fcc, hcp*)
Co/SiO$_2$-35					
350	–	8.4	11.8	–	Co(*fcc, hcp*), CoO
400	–	9.5	13.2	–	Co(*fcc, hcp*), CoO
450	9.0	9.8	10.1	0.3533 (5)	Co(*fcc, hcp*), CoO
510	–	8.2	12.1	–	Co(*fcc, hcp*)
550	–	11.0	9.0	–	Co(*fcc, hcp*)
600	–	10.5	9.5	–	Co(*fcc, hcp*)
700	12.0	10.6	9.4	0.3533 (5)	Co(*fcc*)
800	–	14.5	6.9	–	Co(*fcc*)
900	16.0	17.8	5.6	0.3523 (5)[e]	Co(*fcc*)

[a] % Dispersion calculated from TEM results assuming spherical shape of Co particles.
[b] Lattice constant for Co(*fcc*) $a = 0.3545$ nm (JCPDS file 15-0806).
[c] From XRD only Co(*fcc*) was identified.
[d] After 2 days in air, without paraffin.
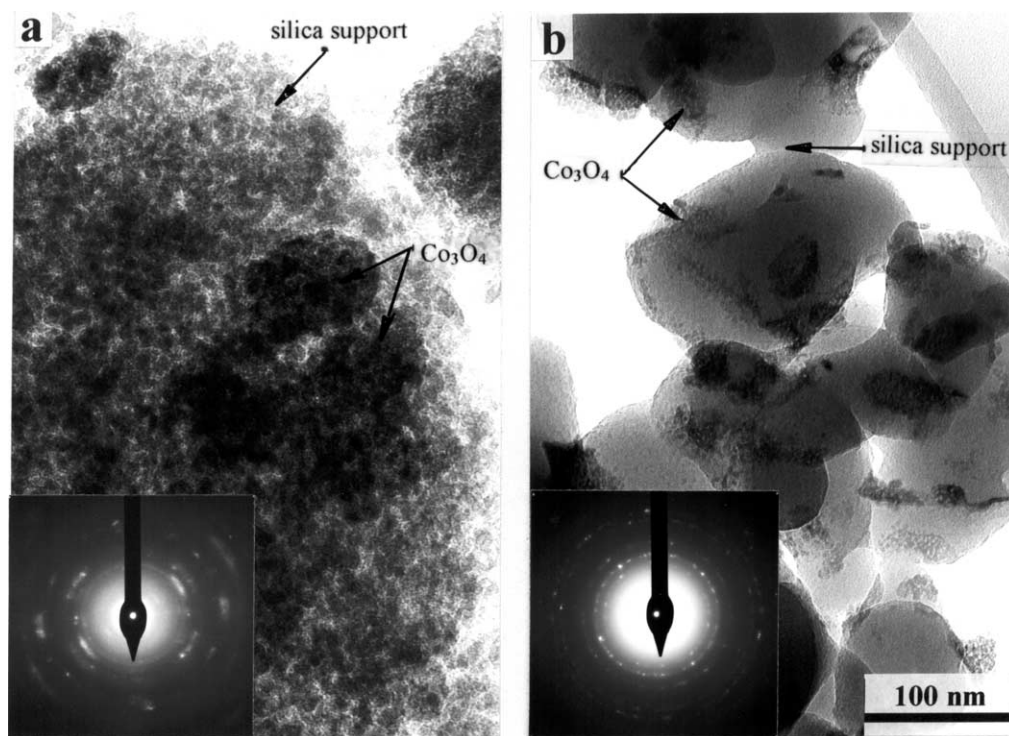[e] Measured without internal standard.

Fig. 2. TEM micrographs of the (a) Co/SiO$_2$-390 and (b) Co/SiO$_2$-35 catalysts after room temperature drying in air for 72 h followed by open air heating at 130 °C for 20 h.
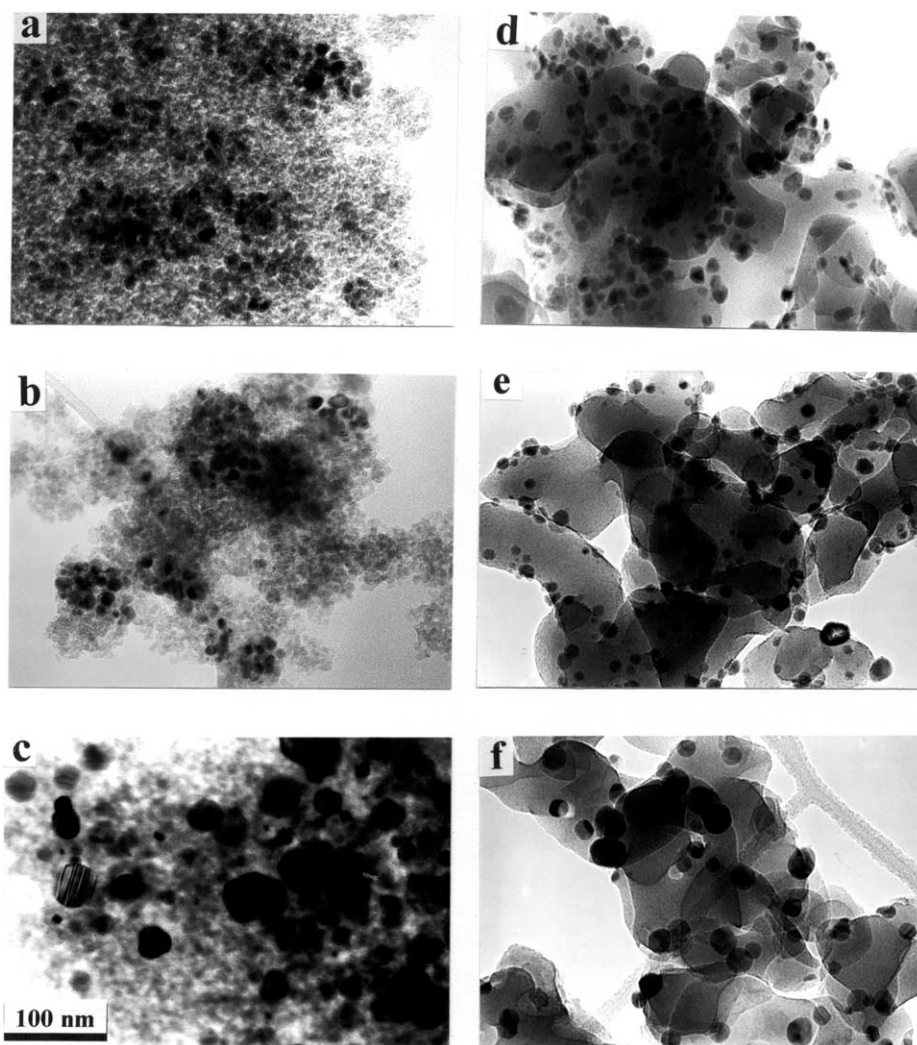
Fig. 3. Series of TEM micrographs of the Co/SiO$_2$-390 (a,b,c) and Co/SiO$_2$-35 (d,e,f) catalysts after reduction for 20 h at 400 (a,d), 700 (b,e), and 900 °C (c,f), respectively. All figures are at the same scale, magnification: 195,000×.

(Fig. 2a), Co$_3$O$_4$ deposits are agglomerated in the form of grape-like or cracked drop-like structures. The distribution of the Co$_3$O$_4$ phase is similar to that reported earlier for Co/SiO$_2$ catalysts prepared with silica carriers of comparable porosity and surface area [20,22,69]. For the low surface area silica (Fig. 2b), the cobalt oxide phase seems to be more uniformly distributed on the support surface in the form of agglomerated drop-like and linear structures, cracked into smaller ones. Note the morphological differences between the supports. In Fig. 3, the TEM images of both Co/SiO$_2$ catalysts reduced at 400, 700, and 900 °C for 20 h are shown. In the samples reduced at 400 and 700 °C, metal particles are agglomerated in grape-like structures for the Co/SiO$_2$-390 catalyst (Fig. 3a), while the Co/SiO$_2$-35 Co particles are rather uniformly distributed all over the support surface (Fig. 3d). The cobalt particle sizes did not show any remarkable differences after reduction at 400 and 700 °C. The reduction of both catalysts at 900 °C led to the growth at cobalt particles (Figs. 3c and 3f) in line with BET surface area decreasing. In Fig. 4 a TEM micrograph of the Co/SiO$_2$-

35 catalyst after reduction at 700 °C is presented. It reveals that cobalt particles are covered with an amorphous adlayer, probably SiO$_x$ or SiO$_2$ migrating onto the particles. For the Co/SiO$_2$-390 catalyst, formation of such an adlayer on Co particles was also observed. At higher reduction temperatures a thicker layer was formed.

The SAED patterns from nearly all studied samples, regardless of the reduction temperature applied, show the presence of both fcc and hcp Co phases (Table 2). In Fig. 5, as an example, the SAED patterns of the Co/SiO$_2$-390 catalyst reduced at 450 and 850 °C are shown, where both Co phases are present. This is in contrast to the XRD results, where only the Co (fcc) phase was found. At reduction temperatures up to 500 °C, some surface oxidation of Co also occurs, since the CoO phase could be also identified in the SAED patterns.

Table 2 presents the influence of the reduction temperature on the cobalt particle sizes and phase composition of both catalysts studied, obtained by using TEM and XRD methods. Data on Co dispersion calculated from TEM are
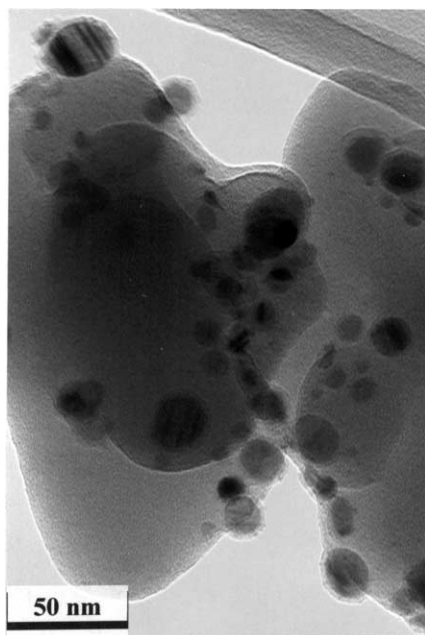
Fig. 4. TEM micrograph of the Co/SiO$_2$-35 catalyst reduced for 20 h at 700 °C. Encapsulation of cobalt particles is visible.

also included. For both catalysts, the mean cobalt particle size varied only slightly with the temperature of reduction. Practically no change occurred up to 800 °C for the Co/SiO$_2$-390 catalyst and up to 700 °C for the Co/SiO$_2$-35 catalyst, while at higher temperatures remarkable growth was observed. It should be noted, however, that the mean cobalt particle sizes obtained from TEM, especially for lower reduction temperatures, could be slightly different from the true ones, due to partial oxidation of the cobalt particles during passivation and handling on air before TEM investigation.

3.4. Magnetic measurements

As it is seen from the data in Table 3 we have not observed any drop of magnetization of the reduced Co/SiO$_2$

catalyst samples which would be expected if the Co–Si solid solution or cobalt silicides were formed. The magnetic moment of Co^0 atoms in the samples of both catalysts reduced at 400 °C is equal to about 1.71 μ_B. The data in Table 3 confirm the total reduction of cobalt species in the catalysts in the whole range of reduction temperatures applied. The metal contents for samples reduced at 700 and 900 °C were higher than those found by standard chemical analysis, and gave apparent reduction degrees between 107 and 114%. For these samples the magnetic moment of the Co^0 atom similarly exhibited an apparent growth by the same magnitude. The correctness of magnetic determination of cobalt contents was additionally verified by chemical titration of cobalt with α-nitro-β-naphthol. The content of the reduced cobalt and its reduction degree in the samples studied by magnetic measurements were simultaneously determined in the O$_2$ uptake experiments. The results of magnetic measurements agree well with oxygen uptake data giving a cobalt reduction close to 100%. The samples reduced at different temperatures exhibited different resistance to oxidation upon exposure to air manifested by a decrease of magnetization (see Fig. 6). An especially large change of magnetization was observed for the catalysts reduced at 350–450 °C, while for the samples reduced at 700 °C this effect was significantly smaller and nearly negligible for the catalysts reduced at 900 °C.

3.5. Oxygen uptake

The oxygen uptake results for the reduced Co/silica catalyst samples are listed in Table 3 together with magnetic data. The degree of Co reduction is close to 100%, in the temperature range studied, irrespective of the reduction temperature applied and silica support used. For the samples reduced at 700 and 900 °C, apparent reduction degrees higher than 100% were found. An important finding is that the oxygen uptakes measured at room temperature for the catalysts reduced at various temperatures differ significantly and decrease with increasing reduction temperature. For the sam-
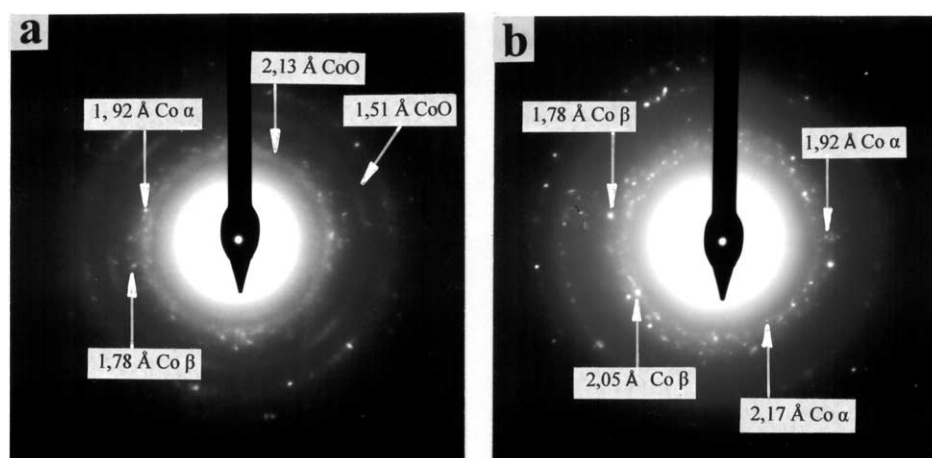

Fig. 5. SAED patterns of the Co/SiO$_2$-390 catalyst reduced for 20 h at (a) 450 °C and (b) 850 °C.

Table 3
Oxygen uptake and magnetic measurements of reduction degrees of Co/SiO_2 catalysts as a function of reduction temperature

Reduction temperature (°C)	Oxygen uptake				Magnetization measurements		
	Total uptake[a] ($\mu mol\ g_{cat}^{-1}$)	Uptake at room temperature (% of total)	Co content[b] (wt%)	Reduction degree[c] (%)	Magnetization σ_s cat. ($emu\ g_{cat}^{-1}$)	Co content[d] (wt%)	Reduction degree[e] (%)
			Co/SiO_2-390				
400[f]	975.8	58	8.54	101	13.9	8.57	100.3
550	985.4	33	–	102	14.3	8.62	103.2
700	1007.6	15	9.0	104.3	14.9	9.19	107.3
900	1081.0	6.5	9.25	111.9	15.7	9.70	113.6
900[f]	1051.1	8	9.1	108.8	–	–	–
			Co/SiO_2-35				
400	553.9	61	4.88	100.3	7.9	4.87	99.8
700	610.0	14.5	5.32	110.5	8.86	5.46	111.9

[a] Uptake after correction on the bare support; measured after oxidation at 450 °C.
[b] Titrated after oxidation at 450 °C.
[c] Calculated from experimentally found oxygen uptake and those theoretically predicted, assuming Co content 8.54 and 4.88 wt% for Co/SiO_2-390 and Co/SiO_2-35, respectively.
[d] Estimated from σ_s cat. measured (extrapolated), assuming σ_s for pure metallic Co = 162.2 emu/g.
[e] Calculated from Co contents found from magnetization and those from standard analysis.
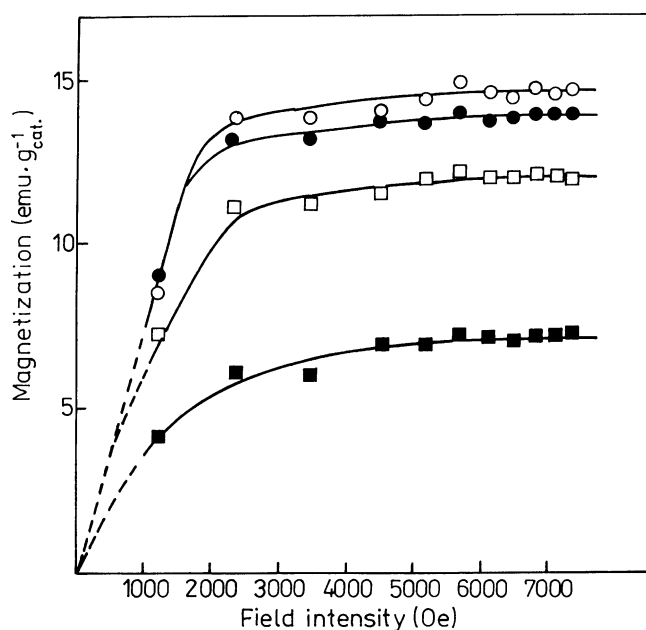[f] Sample handled in air.

Fig. 6. Magnetization curves versus magnetic field intensity for the Co/SiO_2-390 catalyst reduced at (■, □) 400, and (●, ○) 700 °C. Filled symbols represent samples exposed to air and open ones, the catalysts without any contact with air.

ples reduced at 350–500 °C, O_2 uptake amounts to 60% of the total oxygen needed for Co_3O_4 formation, whereas for the samples reduced at 700 and 900 °C it amounts to only 15% or even 7%, respectively. A more detailed presentation of the results on oxygen uptake and magnetic measurements will be given elsewhere.

3.6. Hydrogen chemisorption

The results of hydrogen chemisorption for the Co/SiO_2 catalysts reduced at 400, 550, and 700 °C are shown in Table 4 together with the activity data. The overall dispersion and the average Co metal particle size calculated on the basis of chemisorption data are also given. The results indicate that overall dispersion decreases with increasing reduction temperatures for both catalysts studied. However, the dispersion as well as the cobalt particle sizes found from H_2 uptake differs considerably from those obtained from TEM and XRD measurements, especially for the catalysts reduced at 550 °C. For the samples reduced at 700 °C and higher, the hydrogen chemisorption was unmeasurable.

3.7. Catalytic activity measurements

Fig. 7 shows benzene conversion to cyclohexane as a function of time on stream at 119 °C, measured for the Co/SiO_2-35 catalyst reduced at 450 and 550 °C. Some deactivation of the catalysts with time on stream occurs, especially large during the first 10 min on stream. The effect was more pronounced for the sample reduced at higher temperatures. A similar change of benzene conversion was also observed for the Co/SiO_2-390 catalyst. To compare the catalytic activity of both catalysts reduced in the temperature range of 350–900 °C and not disturbed by major modification of the cobalt particle surfaces, it is reasonable to take into consideration the activity measured before significant deactivation of the catalysts. Hence, as the initial activity we assumed that measured after 20 min on stream. The true initial activities found by extrapolation of the reciprocal of

Table 4
Hydrogen chemisorption and activity for benzene hydrogenation on Co/SiO$_2$ catalysts as a function of reduction temperature

Reduction temperature (°C)	Hydrogen chemisorption			Activity[c]	
	Total uptake (μmol g$_{cat}^{-1}$)	Dispersion[a] (%)	Particle size[b] D (nm)	Reaction rate (μmol g$_{cat}^{-1}$ s^{-1})	TOF[d] (s^{-1})
		Co/SiO$_2$-390			
350	–	–	–	57.4	–
400	47.5	6.8	11.8	59.2	0.62
450	–	–	–	61.3	–
500	–	–	–	43.3	–
550	10.0	1.4	67.0	12.3	0.61
600	–	–	–	7.7	–
700	n.m.[e]	–	–	n.m.	–
800	–	–	–	n.m.	–
900	–	–	–	n.m.	–
		Co/SiO$_2$-35			
350	–	–	–	22.9	–
400	23.0	5.4	14.9	27.6	0.60
450	–	–	–	28.8	–
510	–	–	–	16.7	–
550	7.3	1.7	55.9	9.3	0.63
600	–	–	–	0.9	–
700	n.m.	–	–	n.m.	–
800	–	–	–	n.m.	–

[a] % Dispersion (i.e., percentage exposed to the surface) calculated from % $D = 1.179\ X/Wf$, where X = total H$_2$ uptake, W = wt% Co, $f = 1$ (i.e., fraction of cobalt reduced to the metal).

[b] Calculated assuming 12.2 Co atoms/nm^2 for 400°C [25] and 14.6 for 550° [66].

[c] Activity after 20 min on stream. Reaction conditions: 119°C, H$_2$/benzene ratio 1/8.75, total flow 75 ml/min.

[d] TOF (molecules of benzene reacted per surface Co per second).
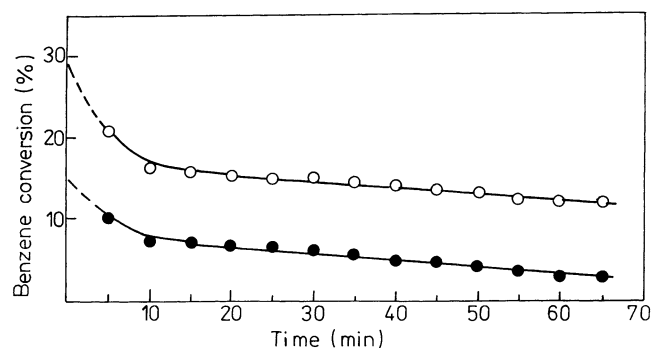
[e] n.m., nonmeasurable.

Fig. 7. Benzene conversion versus time on stream for the Co/SiO$_2$-35 catalyst reduced at: (○) 450 °C, $m_{cat} = 30$ mg, and (●) 550 °C, $m_{cat} = 50$ mg.

activity to time zero [70,71] reflect the same trend as those measured after 20 min on stream.

The influence of the reduction temperature on the catalytic activity of all Co/SiO$_2$ catalysts studied is shown in Fig. 8. The activity results are also summarized in Table 4. Hydrogenation activity of both catalysts increases slowly with the reduction temperature up to 450 °C and then sharply declines to zero for reduction temperatures equal or higher than 600 °C. From the results presented it appears that activity of the Co/SiO$_2$-390 catalyst is higher than that of
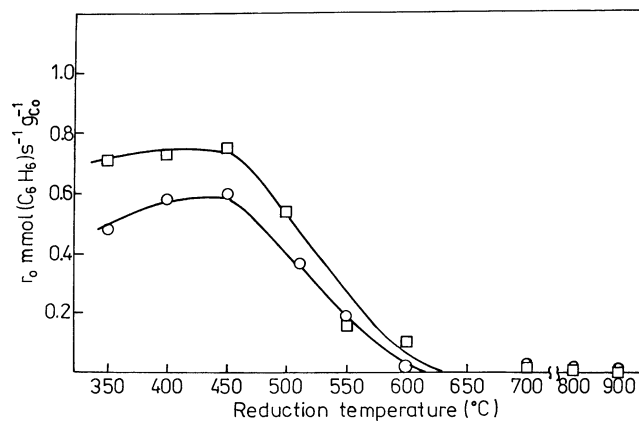
Fig. 8. The effect of reduction temperature of the Co/SiO$_2$ catalysts on benzene hydrogenation at 119 °C; (□) Co/SiO$_2$-390 and (○) Co/SiO$_2$-35.

Co/SiO$_2$-35 catalyst. It means that the amount of active sites in the high surface area Co catalyst is also higher. The turnover frequencies (TOF) calculated on the basis of catalytic activity and hydrogen chemisorption data remain constant, within the limit of experimental error (see Table 4, last column).

4. Discussion

The BET surface areas of the catalysts and supports did not change significantly after various pretreatments at temperatures below 900 °C. Thus, the changes in the catalyst characteristics were not caused by the change in the total surface area except the catalysts reduced at 900 °C where a severe decline of the surface areas occurred.

XRD data indicate that the bare supports and the catalysts treated under hydrogen even at 900 °C, did not undergo recrystallization to quartz or crystobalite. This behavior differs from that observed for catalysts prepared from cobalt acetate or nitrate where after heating in flowing inert gases or oxygen, cobalt silicate formation occurred simultaneously with the crystallization of the same type of silica [43]. After impregnation and drying at room temperature both catalysts, as shown by XRD and TEM, did not contain any crystalline cobalt nitrate phase, probably due to its high dispersion and/or uniform distribution all over the support surface. Uniform distribution of the Co(NO$_3$)$_2$ phase and its migration on the outer surface of silica during the calcination was reported by Castner et al. [69] and recently by Niemelä et al. [72]. After heating at 130 °C in air only the Co$_3$O$_4$ phase was present. Ho et al. [32] and Jongsomjit et al. [34] also reported the Co$_3$O$_4$ formation during heating the cobalt nitrate-derived Co/SiO$_2$ and Co/γ-Al$_2$O$_3$ catalysts at 100 °C for 300 h and 110 °C for 12 h, respectively. The mean crystallite sizes of Co$_3$O$_4$ found from XRD and confirmed by TEM, i.e., about 9.5 and 5 nm for porous and nonporous silicas, respectively, agree well with those usually reported in the literature for silica of similar porosity [21,22,32,69,72]. Our XRD data revealed the formation of

exclusively a Co fcc phase in the catalysts reduced at 350–900 °C and passivated at room temperature. However, in situ XRD studies [25,73] proved the formation of the Co hcp phase also at 350 or even 450 °C, i.e., above the Co phase-transition temperature (422 °C). Srinivasan et al. [25] estimated the Co hcp:Co fcc ratio as 7:3 for the Co/SiO$_2$ catalyst prepared from cobalt nitrate precursors and reduced at 350 °C. Enache et al. [73] studying Co/ZrO$_2$ and Co/Al$_2$O$_3$ catalysts did not detect any metallic Co at 350 °C, whereas at 450 °C various Co hcp:fcc ratios were found depending on the pretreatment. Haddad and Goodwin [45] reported besides Co also Co$_2$O$_3$ and Co$_3$O$_4$ formation for the reduced and passivated 20 wt% Co/SiO$_2$ catalyst. In our experiment, some parts of smaller Co particles could be oxidized (see oxygen uptake) and escape XRD detection [74]. It can be noted, however, that our SAED patterns from nearly all catalysts studied revealed only Co hcp and Co fcc formation, and at lower reduction temperatures (up to 500 °C) a small amount of poorly crystallized CoO was also detected. The catalysts reduced at higher temperatures exhibited higher resistance to oxidation, since no CoO was observed by TEM and XRD. A similar phase composition was also observed by TEM in thin cobalt films evaporated on a silica support [57]. The population of Co hcp particles, roughly estimated from TEM for both catalysts reduced at 350–400 °C, was higher than Co fcc. At higher temperatures, in agreement with the Co phase diagram, mainly the Co fcc phase was observed. However, for the Co/SiO$_2$-390 catalyst a single, Co hcp particle could still be observed by TEM even at 900 °C, whereas for Co/SiO$_2$-35 only the Co fcc phase was present above 700 °C (cf. Table 2).

The cobalt crystallite size determined from XRD and TEM remains nearly unchanged up to 700 °C for Co/SiO$_2$-35 and to 800 °C for Co/SiO$_2$-390 catalysts. However, the intensity of the XRD peak of (111) Co fcc significantly rises with the temperature of reduction, which confirms the growing resistance of Co to oxidation. This phenomenon can be the explained by cobalt particle encapsulation and/or formation of better crystallized cobalt particles more resistant to oxygen. In fact, as it was shown by TEM, in the Co/SiO$_2$ catalysts reduced at 700 °C and above, the cobalt particles are covered with a 2–3-nm thick amorphous layer of another material most probably SiO$_2$ or SiO$_x$ (Fig. 5). Such silica migration is possible and strongly depends on the presence of water vapor [13,36,56]. Also, our oxygen uptake and magnetic measurements confirm the idea of the protective silica layer formation. On the other hand the migration of silica is intensified because a large change of BET surface area was observed and an encapsulation of cobalt particles with a thicker support layer took place. It might be worth noting that cobalt particles formed during the cobalt silicate reduction showed a similar resistance to oxidation [43]. The lack of sintering of Co particles up to 800 °C in the case of the SiO$_2$-390 support could be explained as a result of diffusion constraints due to the porosity of the support. The mean diameter of Co particles (8–10 nm) is nearly the same as the

mean pore diameter of this support. This agrees well with finding of Castner et al. [13] who reported that the Co particle size strongly depends on the mean pore diameter of the silica support. For low surface area silica such geometrical constraints do not exist; nevertheless, the sizes of cobalt particles remain practically constant up to 700 °C. It seems that strong interaction with the support maintains the Co particles in place.

The lattice parameter of Co (fcc), measured with the use of silicon as an internal standard, for the reduced catalysts, showed a decrease of 0.26% as compared to the JCPDS file (15-0806) data (see Table 2). This effect could be due either to the Co–Si solid solution formation [75] or to oxygen chemisorption [76] since both processes induce a similar decrease of the lattice parameter. In the case of Co–Si solid solution formation such lattice contraction could correspond roughly to about 12 at.% of Si in cobalt [75].

It is known that the magnetic method allows the determination of ferromagnetic metal contents [28,77]. It can be used also to study alloying [16,78] or solid solution formation [79], especially when one of the components is ferromagnetic. If the Co–Si solid solution were formed it should result in a significant drop of magnetization. Pearsons et al. [80] reported the drop of a magnetic moment of the cobalt atom from 1.71 to 1.62 μ_B and 1.49 μ_B for the bulk solid solution containing 2.26 and 4.57 at.% of Si, respectively. With the Co$_2$Si or other silicides formation a drop of magnetization or even paramagnetism should be observed [80–82]. In our study all samples exhibited only ferromagnetic Co behavior (Table 3), which agrees well with TEM and XRD data showing the cobalt particle sizes above of those predicted for superparamagnetic ones [77]. Also the magnetic moment of cobalt atoms equal to 1.71 μ_B found for the Co/SiO$_2$ catalyst samples reduced at 400 °C exactly matches the literature data for ferromagnetic cobalt [77]. It is seen that the magnetic results presented clearly excluded the possibility of Co–Si solid solution formation that lowered the magnetization and magnetic moment of Co atoms [80]. Praliaud and Martin [79] for Ni/SiO$_2$ catalysts reduced at high temperature observed such a decrease of magnetization. The metal contents found by the magnetic method confirmed the total reduction of Co in all studied samples (cf. Table 3). For both catalysts reduced at 700 and 900 °C, similarly as in O$_2$ uptake, apparent reduction degrees higher than 100% were found. Such high, apparent reduction degrees, namely 115% for Co/SiO$_2$ catalysts reduced at 650 °C, and a superparamagnetic cobalt formation were also reported by Barbier et al. [28] for cobalt/silica catalysts prepared by the ammonia method. They suggested that this effect could be due to the presence of a residual phyllosilicate or silicate containing Co^{2+} ions, thus giving the growth of magnetization (the magnetic moment of Co^{2+} (5 μ_B) is nearly three times as large as that of Co^0 atoms). However, on the basis of our oxygen uptake and magnetic and chemical titration results, we claim that this effect is due rather to the support mass loss via its dehydroxylation and/or partial reduction [48,83].

Comparing the cobalt contents found from magnetic measurements and oxygen uptake data it appears that at all reduction temperatures applied we achieve a 100% Co reduction. Moreover, nearly equal magnitudes of magnetization found at 77 and 298 K suggests the presence of only a ferromagnetic Co phase, since a lack of temperature dependence of magnetization—typical for paramagnetic Co^{2+} ion—was observed. Some very small support reduction could not be, however, excluded. Magnetic measurements confirmed also a grater resistance to oxidation of the samples reduced at higher temperatures observed in this study with other methods.

Oxygen uptake primarily was used as a tool for determination of the degree of cobalt reduction. Unexpectedly, it provided additional information on the resistance of cobalt particles to oxidation. In order to exclude the possible effect of exposure of the reduced catalysts to air we had experiments with the samples prepared with and without contact with air. Our results showed that these two kinds of the experiments give essentially the same results. This could be interpreted as an evidence of the lack of any substantial reduction of the support to Si or SiO_x species highly sensitive to oxygen. The O_2 uptake data showed that reduction with hydrogen for 20 h at 350 °C was sufficient for the total reduction of cobalt in both Co/SiO_2 catalysts. It agrees well with the results of Hercules and co-workers [32] and Castner et al. [69] who reported the complete Co reduction in the catalysts at 350–400 °C. The samples reduced at 700 and 900 °C revealed an oxygen consumption higher than 100%; i.e., the apparent reduction degrees (O_2 measured/O_2 theoretically calculated on the basis of standard chemical titration) varied between 104 and 112% (cf. Table 4). This could be due to the support mass loss caused by severe dehydroxylation and/or its partial reduction. Jóźwiak et al. [83] analyzing thermogravimetric profile have shown that silica heated from 200 up to 1100 °C releases water loosing 3.49 wt% of its mass. Oxygen consumption higher than 100% should also be expected in the case of partial reduction of the support. Also the formation of the Co–Si solid solution, assuming its oxidation to Co_3O_4 and SiO_2, could also force the higher oxygen consumption; however, this possibility was excluded. In fact, the cobalt titration in these samples performed directly after oxygen uptake experiments revealed Co contents higher than that obtained from standard analysis in the initial samples, thus confirming the severe support mass loss during the reduction. This means that simple reoxidation at 450 °C is insufficient to restore the initial formula of the catalyst (cf. Table 3). Kunimori et al. [84], however, have shown that a Pt/TiO_2 catalyst, reduced at 500 °C, in the SMSI state was able to restore its initial formula and chemisorptive properties when treated under oxygen at 400 °C. Samples of Co/SiO_2 reduced at 350–500 °C and then exposed to oxygen at room temperature consumed up to 60% of the oxygen needed for Co_3O_4 formation. For the range 550–600 °C the O_2 consumption was about 33–35% of the theoretical one. The samples reduced at 700 and 900 °C consumed about 15 and 7%, respectively. Taking into account the negligible change of the mean cobalt particle sizes for catalysts reduced at 400 and 700 °C, or even at 800 °C for the Co/SiO_2-390 catalyst, it is evident, that there must be some kind of coverage of cobalt particles, or formation of a surface compound, which stops or hinders oxygen penetration into the cobalt particles. For these samples to achieve faster oxygen consumption during the uptake experiment it was necessary to raise the temperature up to about 180 °C. Probably in these samples the leakage or diffusion of oxygen into metallic cobalt goes through the cracks in the silica layer or noncovered part of the particles surfaces and therefore the growth of the temperature is needed to significantly accelerate the velocity of diffusion.

Our H_2 chemisorption data show a significant decrease of the Co dispersion and particle size growth with increasing temperature of reduction for both catalysts. For temperatures higher than 600 °C the chemisorption of hydrogen was practically nonmeasurable (Table 4). However, our TEM and XRD data indicate that H_2 chemisorption is a rather inappropriate method for the calculation of a mean particle size in cobalt/silica catalysts reduced at $T \geqslant 500$ °C. On the other hand it is a good measure of the number of cobalt atoms or surface area available to the reaction. The H_2 chemisorption change seems to follow the change observed for catalyst activity in benzene hydrogenation. The mean cobalt particle size and dispersion determined on the basis of hydrogen chemisorption, at least for Co/SiO_2 catalyst reduced at $T > 450$ °C, should be considered as "apparent" or "effective" rather than as real ones. Reuel and Bartholomew [67] also suggested that at higher reduction temperatures when strong metal-support interaction occurs, H_2 uptake measurement do not reflect the true Co surface area and particle size. Nevertheless, H_2 chemisorption is commonly used for determination of Co dispersion and crystallite size, and the decrease of H_2 chemisorption is most likely inappropriately interpreted as the effect of the agglomeration of cobalt particles [85]. The suppression of H_2 chemisorption is, as discussed above, the result of SMSI effect. Benzene hydrogenation was also proposed as a method for metal surface area measurements, especially in the systems in which support-metal interactions are expected to occur [71]. However, we could not use this method, because of significant deactivation of the catalysts (Fig. 6).

We found that activity of Co/SiO_2-390 catalyst was slightly higher than the Co/SiO_2-35. It is due to the fact that the increase in the support surface area led to some improvement of the metal dispersion found also by H_2 chemisorption. The activity of both catalysts first increased slowly reaching a maximum for reduction temperature of 450 °C, and then sharply declined to zero for about 600 °C. The lower activity of the samples reduced at 350–400 °C was probably caused by the different Co hcp and fcc phase population. The average number of the exposed Co atoms is 11.3 and 14.6/mn^2 for hcp and fcc phases, respectively [67].

A decrease in the amount of active Co metal sites available for reaction was accompanied by a decrease of H_2 chemisorption (cf. Table 4). The TOF for hydrogenation of benzene, calculated from the total hydrogen chemisorption, was the same for both Co/SiO_2 catalysts reduced at 400 and 550 °C and nearly independent of the silica used. It is likely that this finding confirms that the hydrogenation of benzene on Co/SiO_2 catalysts is a structure-insensitive reaction, similarly as on other metals [3,62], with particle sizes similar to those used in this study. Literature data on the reaction of benzene with hydrogen on cobalt catalyst are rather scarce [6–8,59,60,86] and we were not able to find other TOF data to compare with ours. Taylor and Staffin [6] found that the specific activity of benzene hydrogenation on supported Co is independent of the particle size and support material (silica, alumina, silica-alumina). Iglesia et al. [87] found that hydrocarbon synthesis (FT) on supported Co was also proportional to metal dispersion and almost independent of the support.

As a possible explanation for the decrease of specific activity of both catalysts, the sintering of Co particles due to the reduction at $T \geqslant 500$ °C cannot be considered (see Table 2). The changes in the activity are not caused by incomplete Co reduction, because all Co present on both supports was reduced to the metallic state, as was confirmed by the O_2 uptake and magnetic results. The data of Tables 2 and 4 indicate that only a part of the Co detected by XRD and TEM was available for hydrogen adsorption. This observation and decrease of the catalytic activity suggest that reduction at $T \geqslant 500$ °C induces enhanced interaction between the cobalt and the silica support, probably involving migration of the SiO_2 support onto the reduced Co particles. Zadeh and Smith [88] also observed significant differences in dispersion as estimated by XRD and H_2 chemisorption for the Co/SiO_2 catalyst and attributed it to the decoration of Co by SiO_2. Ho et al. [8] reported for titania supported cobalt, that decoration effects decreased the activity in benzene and CO hydrogenation. The decrease of activity for benzene hydrogenation was also observed for the Pt/SiO_2 catalyst reduced at 500 °C and was explained by some degree of encapsulation of the platinum particles by the silica support [89]. For the catalysts reduced at 600 °C or above, a drastic decrease of activity and suppression of H_2 chemisorption was observed. Results may be explained by the complete decoration of Co particles by SiO_2 or by electronic effects on cobalt due to the partial reduction of the support. The decrease of catalyst activity due to the formation of Co–Si solid solution or Co silicides, as stated above, is excluded. In an earlier paper [60] we have found that O_2 treatment of the Co/SiO_2-35 catalyst reduced at 600 °C followed by a low-temperature reduction was not capable of restoring the hydrogenation activity of the catalyst. This finding and the present data confirm the strong influence of the support on the activity of both catalysts studied. Niemelä et al. [85] reported that the $Co(N)/SiO_2$ catalyst was the most active for toluene hydrogenation af-

ter reduction at 300 °C and almost inactive after reduction at 500 °C. The change of activity was interpreted, however, as the effect of Co agglomeration. Decrease of activity has been observed also for Ni/SiO_2 catalysts reduced at high temperatures [79,90]. On the other hand, Ruckenstein and Wang [4] observed that 12 wt% Co/SiO_2 catalyst reduced at 900 °C was active in CO_2 reforming of methane even at 900 °C. It seems that the conditions of the reduction, especially water vapor removal, strongly influence the final catalyst activity.

The possible cobalt–silica interactions—as it was pointed out in Introduction—may be of various origins. The first one, i.e., cobalt hydrosilicate/silicate formation, can be expected during the first stage (impregnation, drying, calcination) of cobalt catalyst preparation. This effect is claimed to be a reason for the lowering of the degree of cobalt reduction. This type of interaction is avoided in our experiments, since 100% Co reduction was achieved even at 350 °C. Apparently mild calcination treatment adopted here does not induce strong interaction of the cobalt phase with silica support [32]. The second type of interaction is claimed to be induced by metallic cobalt via activation of the chemisorbed hydrogen (spillover effect), which may reduce the support to Si atoms consecutively reacting with Co and forming the solid solution or even silicides. Our SAED, XRD, and magnetic results did confirm neither Co–Si solid solution nor Co_2Si formation at least in measurable quantities. However, oxygen uptake data do not exclude a partial reduction of the support to SiO_x species. The cobalt particles encapsulation with migrating silica or partly reduced support moieties can be considered as a third type of a metal support interaction. The silica migration may be induced and strongly influenced by water vapor, which is a by-product of the reduction of oxidic form of Co. As an additional source of water in the system, especially at higher temperatures of reduction, the dehydroxylation of silica can be considered which can also accelerate the silica migration. The silica migration onto Co can also explain the rather high resistance of Co particles to sintering, as the migrating silica species can reinforce the Co–SiO_2 interface forming a stabilizing framing at the bottom side of Co (a kind of glue). In the case of porous system, the pore-stabilizing effect could additionally reinforce this interaction. At temperatures $\geqslant 700$ °C, severe dehydroxylation and/or reduction of the support occurs, as evidenced by abnormally high apparent reduction degrees and the inability of restoring the initial state of the catalyst by the simple reoxidation at 450 °C as confirmed by chemical analysis of the reoxidized samples. The cobalt contents found were still higher than that in the initial sample (cf. Table 3, oxygen uptake). We suppose that in our study the last mechanism of cobalt deactivation, i.e., cobalt crystallite decoration or encapsulation with migrating silica, prevailed and mostly significant at temperatures 500–900 °C. The silica liability toward the water vapor described above can be expected also in other metal/silica systems and is under study in our laboratory.

5. Conclusions

1. Mild calcination treatment of impregnated, cobalt nitrate-derived Co/SiO$_2$ catalysts enables avoiding the strong interaction of the oxidic cobalt phase with silica carriers, both high and low surface area, and thus prevents irreversible cobalt deactivation. It yields a reduction degree of Co close to 100% and produces a medium dispersed cobalt phase.

2. The mean size of cobalt particles remains stable in a very broad range of temperatures and metal sintering occurred at temperature higher than 700 °C for low surface area silica and 800 °C for porous, high surface area silica.

3. Reduction with hydrogen in the temperature range of 350–900 °C produces fcc Co and, to a lower extent, hcp Co phases. For the high surface area silica scarce Co hcp particles were observed even after the reduction at 900 °C. Formation of Co–Si solid solution or Co$_2$Si silicide, postulated in our earlier paper [59], was not confirmed at least, in the detectable quantities.

4. At 500–600 °C, migration of the support species onto Co particles, probably induced by water vapor presence, leads to a partial covering of the cobalt particle with a hardly visible adlayer. This process causes a rapid decrease of chemisorption and catalytic activity of Co metal and growing resistivity to oxidation when exposed to air.

5. At 700 °C, besides the silica migration, also a partial loss of the support weight, probably due to the intense support dehydroxylation and/or reduction, is observed. The process manifests a higher than 100% apparent reduction degree of Co accompanied with a total loss of catalytic activity and chemisorptive capacity. Surface decoration of cobalt particles with a layer of migrating SiO$_2$ or SiO$_x$ species is easy visible in TEM.

6. At 900 °C, severe damage and weight loss of the support take place accompanied by cobalt sintering and a deep encapsulation of cobalt metal crystallites by the collapsing support. In this state the catalyst was barely sensitive to exposure to air.

7. It appears that the use of hydrogen chemisorption for determination of the dispersion and mean particle size of cobalt is limited to temperatures lower than 500 °C, because for higher temperatures, due to the encapsulation of Co crystallites by migrating support, the obtained results can be unreliable.

8. Magnetic and oxygen uptake results indicate that at temperatures higher than 700 °C besides strong silica dehydroxylation, also some support reduction probably to SiO$_x$ occurs. However, the formed protective silica layer, suppressing totally the chemisorption and catalytic activity, is not fully oxygen proof and allows the partial leaking of oxygen into Co crystallites.

Acknowledgments

Appendix A

In our earlier TEM study of Co/SiO$_2$-35 catalysts reduced at or above 700 °C [59], we have suggested on a basis of microdiffraction from few small Co particles the possibility of Co$_2$Si formation. However, the microdiffraction patterns obtained could be ascribed to the faulted Co particles. On the basis of the present study, where a large number of samples and a variety of methods were applied, we thought that the hypothesis of Co–Si solid solution as well as Co$_2$Si formation should be ruled out.

In Ref. [59] by mistake, we specified as the object of investigations the Co/SiO$_2$-390 (XOA-400) instead of Co/SiO$_2$-35 (XOB-15).

References

[1] M.E. Dry, in: J.R. Anderson, M. Boudart (Eds.), Catalysis Sciences and Technology, Vol. 1, Springer, Berlin, 1981, p. 159.
[2] V. Ponec, G.C. Bond, Stud. Surf. Sci. Catal. 95 (1995) 704.
[3] E. Iglesia, Appl. Catal. A 161 (1997) 59;
S. Krishnamoorthy, M. Tu, M.P. Ojeda, D. Pinna, E. Iglesia, J. Catal. 211 (2002) 422.
[4] E. Ruckenstein, H.Y. Wang, Appl. Catal. A 204 (2000) 257.
[5] T.A. Kainulainen, M.K. Niemelä, A.O.I. Krause, Catal. Lett. 53 (1998) 97.
[6] W.F. Taylor, H.K. Staffin, J. Phys. Chem. 71 (1967) 3314.
[7] J. Völter, M. Hermann, K. Heise, J. Catal. 12 (1968) 307.
[8] S.W. Ho, J.M. Cruz, M. Houalla, D.M. Hercules, J. Catal. 135 (1992) 173.
[9] C. Ando, H. Kurokawa, H. Miura, Appl. Catal. A 185 (1999) L181.
[10] R.L. Chin, D.M. Hercules, J. Phys. Chem. 86 (1982) 360.
[11] R.C. Reuel, C.H. Bartholomew, J. Catal. 85 (1984) 78.
[12] G.M. Roe, M.J. Ridd, K.J. Cavell, F.P. Larkins, Stud. Surf. Sci. Catal. 36 (1988) 509.
[13] I.Y. Chan, D.G. Castner, P.R. Watson, J. Phys. Chem. 94 (1990) 819.
[14] I. Puskas, T.H. Fleisch, J.B. Hall, B.L. Meyers, R.T. Rochinski, J. Catal. 134 (1992) 615.
[15] E. Van Steen, G.S. Sewell, R.A. Makhothe, C. Micklethwaite, H. Manstein, M. De Lange, C.T. O`Connor, J. Catal. 162 (1996) 220.
[16] F.B. Noronha, M. Schmal, C. Nicot, B. Moraweck, R. Frety, J. Catal. 168 (1997) 42.
[17] M. Kraum, M. Baerns, Appl. Catal. A 186 (1999) 189.
[18] R. Riva, H. Miessner, R. Vitali, G. Del Piero, Appl. Catal. A 196 (2000) 111.
[19] L.B. Backman, A. Rautiainen, M. Lindblad, A.O.I. Krause, Appl. Catal. A 191 (2000) 55.
[20] M. Voß, D. Borgmann, G. Wedler, J. Catal. 212 (2002) 10.
[21] M.P. Rosynek, C.A. Polansky, Appl. Catal. 73 (1991) 97.
[22] Y. Okamoto, K. Nagata, T. Adachi, T. Imanaka, K. Inamura, T. Takyu, J. Phys. Chem. 95 (1991) 310.
[23] T. Matsuzaki, K. Takeuchi, H. Hanaoka, H. Arakawa, Y. Sugi, Catal. Today 28 (1996) 251.
[24] S. Sun, N. Tsubaki, K. Fujimoto, Appl. Catal. A 202 (2000) 121.
[25] R. Srinivasan, R.J. De Angelis, P.J. Reucroft, A.G. Dhere, J. Bentley, J. Catal. 116 (1989) 144.

[26] H. Ming, B.G. Baker, Appl. Catal. A 123 (1995) 23.

[27] A.Yu. Khodakow, J. Lynch, D. Bazin, D. Rebours, B. Zanier, B. Moisson, P. Chaumette, J. Catal. 168 (1997) 16.

[28] A. Barbier, A. Hanif, J.A. Dalmon, G.A. Martin, Appl. Catal. A 168 (1999) 333.

[29] B. Ernst, S. Libs, P. Chaumette, A. Kiennemann, Appl. Catal. A 186 (1998) 145.

[30] K.E. Coulter, A.G. Sault, J. Catal. 154 (1995) 56.

[31] A. Kogelbauer, J.C. Weber, J.G. Goodwin, Catal. Lett. 34 (1995) 259.

[32] S.W. Ho, M. Houalla, D.M. Hercules, J. Phys. Chem. 94 (1990) 6396.

[33] Y. Zhang, D. Wei, S. Hammache, J.G. Goodwin, J. Catal. 188 (1999) 281.

[34] B. Jongsomjit, J. Panpranot, J.G. Goodwin, J. Catal. 204 (2001) 98.

[35] W. Juszczyk, D. Łomot, J. Pielaszek, Z. Karpiński, Catal. Lett. 78 (2002) 95.

[36] B. Viswanathan, R. Gopalakrishnan, J. Catal. 99 (1986) 342.

[37] S. Ali, B. Chen, J.G. Goodwin, J. Catal. 157 (1995) 35.

[38] D. Schanke, S. Vada, E.A. Blekkan, A.M. Hilmen, A. Hoff, A. Holmen, J. Catal. 156 (1995) 85.

[39] B. Ernst, L. Hilaire, A. Kiennemann, Catal. Today 50 (1999) 413.

[40] N. Tsubaki, S. Sun, K. Fujimoto, J. Catal. 199 (2001) 236.

[41] G.L. Haller, D.E. Resasco, Adv. Catal. 36 (1989) 173.

[42] A. Lapidus, A. Krylova, V. Kazanskii, V. Borovkov, A. Zaitsev, J. Rathousky, A. Zukol, M. Jancalkova, Appl. Catal. 73 (1991) 65.

[43] J.M. Jabłoński, M. Wołcyrz, L. Krajczyk, J. Catal. 173 (1998) 530.

[44] A. Khodakow, O. Ducreux, J. Lynch, B. Rebours, P. Chaumette, Oil Gas Sci. Technol. 54 (1999) 525.

[45] G.J. Haddad, J.G. Goodwin, J. Catal. 157 (1995) 25.

[46] G.W. Huber, C.G. Guymon, T.L. Conrad, B.C. Stephenson, C.H. Bartholomew, Stud. Surf. Sci. Catal. 139 (2001) 423.

[47] S.J. Tauster, S.C. Fung, R.L. Garten, J. Am. Chem. Soc. 100 (1978) 170.

[48] R. Oukaci, D.G. Blackmond, A. Sayari, J.G. Goodwin, S.A. Stevenson, G.B. Raupp, J.A. Dumesic, S.J. Tauster, R.T.K. Baker, in: A. Scott, J.A. Stevenson, R.T.K. Dumesic, E. Baker, E. Ruckenstein (Eds.), Metal–Support Interaction in Catalysis, Sintering and Redispersion, Van Nostrand–Reinhold, New York, 1987, p. 112.

[49] W. Trzebiatowski, W. Romanowski, Bull. Acad. Polon., Ser. Sci. Chim. 8 (1960) 113.

[50] W. Trzebiatowski, H. Kubicka, Z. Chem. 3 (1963) 262.

[51] R. Lamber, N.I. Jaeger, G. Schulz-Ekloff, Surf. Sci. 227 (1990) 268.

[52] L. Kępiński, M. Wołcyrz, J.M. Jabłoński, Appl. Catal. 54 (1989) 267.

[53] R. Lamber, W. Romanowski, J. Catal. 105 (1987) 213.

[54] L. Kępiński, M. Wołcyrz, Appl. Catal. 73 (1991) 173.

[55] R. Lamber, N.I. Jaeger, G. Schulz-Ekloff, J. Catal. 123 (1990) 285.

[56] C.R.F. Lund, J.A. Dumesic, J. Catal. 72 (1981) 21.

[57] D. Potoczna-Petru, L. Kępiński, J. Mater. Sci. 28 (1993) 3501.

[58] D. Potoczna-Petru, Mater. Chem. Phys. 55 (1998) 224.

[59] J.M. Jabłoński, D. Potoczna-Petru, J. Okal, L. Krajczyk, React. Kinet. Catal. Lett. 54 (1995) 15.

[60] D. Potoczna-Petru, J.M. Jabłoński, J. Okal, L. Krajczyk, Appl. Catal. A 175 (1998) 113.

[61] M.K. Niemelä, L. Backman, A.O.I. Krause, T. Vaara, Appl. Catal. A 156 (1997) 319.

[62] M. Che, C.O. Bennet, Adv. Catal. 36 (1989) 55.

[63] G.O. Muller, Praktikum der Quantitativen Chemischen Analyse, S. Hirzel, Leipzig, 1952, p. 225.

[64] P. Gallezot, in: J.R. Anderson, M. Boudart (Eds.), Catalysis Sciences and Technology, Vol. 5, Springer, Berlin, 1984, p. 221.

[65] J.M. Jabłoński, J. Mulak, W. Romanowski, J. Catal. 47 (1977) 147.

[66] C.H. Bartholomew, R.J. Farrauto, J. Catal. 45 (1976) 41.

[67] R.C. Reuel, C.H. Bartholomew, J. Catal. 85 (1984) 63.

[68] B. Sen, M.A. Vannice, J. Catal. 113 (1988) 52.

[69] D.G. Castner, P.R. Watson, I.Y. Chen, J. Phys. Chem. 93 (1989) 3188.

[70] J.E. Germain, R. Maurel, C. R. Acad. Sci. 247 (1958) 1854.

[71] F. Fajardie, J.F. Tempére, G. Djèga-Mariadassou, G. Blanchard, J. Catal. 163 (1996) 77.

[72] M.K. Niemelä, A.O.I. Krause, T. Vaara, J. Lahtinen, Top. Catal. 2 (1995) 45.

[73] D.I. Enache, B. Rebours, M. Roy-Auberger, R. Revel, J. Catal. 205 (2002) 346.

[74] C.R. Brundle, T.J. Chuang, D.W. Rice, Surf. Sci. 60 (1976) 285.

[75] H.L. Luo, P. Duwez, Can. J. Phys. 41 (1963) 758.

[76] Z. Kaszkur, J. Appl. Crystallogr. 33 (2000) 87.

[77] P.W. Selwood, Chemisorption and Magnetization, Academic Press, New York, 1975.

[78] W. Romanowski, Roczniki Chem. 51 (1977) 493.

[79] H. Praliaud, G.A. Martin, J. Catal. 72 (1981) 394.

[80] D. Pearsons, W. Sucksmith, J.E. Thompson, Philos. Mag. 49 (1958) 1174.

[81] R. Benoit, J. Chim. Phys. 52 (1955) 119.

[82] G. Foëx, J. Phys. 9 (1938) 37.

[83] W.K. Jóźwiak, W. Ignaczak, D. Kincel, J. Góralski, T. Paryjczak, Polish. J. Chem. 76 (2002) 857.

[84] K. Kunimori, S. Matsui, T. Uchijima, J. Catal. 85 (1984) 253.

[85] M.K. Niemelä, L. Backman, A.O.I. Krause, T. Vaara, Appl. Catal. A 156 (1997) 319.

[86] W.F. Taylor, J. Catal. 9 (1967) 999.

[87] E. Iglesia, S.L. Soled, R.A. Fiato, J. Catal. 137 (1992) 212.

[88] J.S.M. Zadeh, K.J. Smith, J. Catal. 176 (1998) 115.

[89] A. Sepúlveda-Escribano, F. Coloma, F. Rodriguez-Reinoso, J. Catal. 178 (1998) 649.

[90] G.A. Martin, J.A. Dalmon, React. Kinet. Catal. Lett. 16 (1981) 325.